Application of the local plasma approximation for atomic generalised oscillator strengths

1988 J. Phys. B: At. Mol. Opt. Phys. 21 2901

(http://iopscience.iop.org/0953-4075/21/16/015)

J. Phys. B: At. Mol. Opt. Phys. 21 (1988) 2901-2912. Printed in the UK

Application of the local plasma approximation for atomic generalised oscillator strengths†

C M Kwei‡, T L Lin‡ and C J Tung§

‡ Department of Electronics Engineering, National Chiao Tung University, Hsinchu, Taiwan

§ Institute of Nuclear Science, National Tsing Hua University, Hsinchu, Taiwan

Abstract. Generalised oscillator strengths of atoms for inelastic interactions have been calculated based on a local plasma approximation. Determinations of the effective oscillation frequency associated with the electron density of a given subshell and at a given location in an atom have been made. The electron density distribution obtained from the Hartree-Fock-Slater model was utilised. The local plasma oscillation was evaluated with and without plasma dampings. Calculated results of the generalised oscillator strength for several atoms have been compared with other theoretical data. Fairly reasonable agreement was found.

1. Introduction

Penetration of charged particles in matter has been the subject of numerous investigations since the early work of Lenard (1895), Bragg and Kleeman (1905), Rutherford (1911) and Thompson (1912), because of its importance in such areas as radiology, astrophysics, nuclear physics, solid-state physics, radiation physics, etc.

Following the classical and semiclassical treatments of atomic collisions with charged particles, Bethe (1930, 1933) dealt with the problem by a quantum mechanical procedure using the first Born approximation. He considered the transfers of momentum and energy as a result of the inelastic collision between an incident charged particle and an atom and derived the collision cross section in terms of the generalised oscillator strength (GOS). The GOS introduced by Bethe characterises the dynamical response properties of an atom to the interacting charged particle. This quantity is closely related to the energy loss function of condensed matter. In the case of a weakly interacting atomic system such as a dilute gas, the following approximate relation holds (Fano 1963):

$$\frac{\mathrm{d}f}{\mathrm{d}W}=\frac{2WZ}{\pi W_{\mathrm{p}}^2}\,\mathrm{Im}\left(-\frac{1}{\varepsilon(W)}\right) \tag{1}$$

where $\mathrm{d}f/\mathrm{d}W$ is the GOS of a constituent atom, $\mathrm{Im}(-1/\varepsilon)$ is the energy loss function of the system, W is the excitation energy, W_{p} is the free electron plasma energy (as if electrons in the system were free), and Z is the atomic number. Note that atomic units are used in this paper unless otherwise specified.

According to Bethe's definition, the GOS is expressed in terms of the transition matrix element involving initial and final eigenstates of an atom. Detailed atomic

† Research sponsored by the National Science Council of the Republic of China.

0953-4075/88/162901+12$02.50

wavefunctions must be known in order to calculate the GOS. This task is fairly tedious and difficult and thus limits its application. Lindhard and Scharff (1953) proposed a statistical model, later referred to as the local plasma approximation (LPA), using the concept of an inhomogeneous free electron gas to describe the collective oscillation of the electron density at any location in an atom. In this approximation, it was considered that the plasma oscillation of the electron cloud around the nucleus played an equally important role to the individual revolution of electrons in contributing to the dynamical response of an atom in the stopping medium. Since the advent of the LPA, it has been explored in several applications to verify its simplicity and usefulness (Chu and Powers 1972, Tung *et al* 1979, Tung and Watt 1985, Tung and Kwei 1985).

In this paper, we will first try to study the LPA through a mathematical formulation based on a single group of bound electrons corresponding to a single subshell in an atom of a dilute gas. Generalisation of the LPA to a system composed of several subshells of correlated electron densities will follow next. We will then apply the LPA to formulate atomic GOS both considering and neglecting the plasma damping effect. Finally, we will present and discuss the results of GOS for several atoms calculated using the LPA and compare these results with those obtained using the more detailed method.

2. Theoretical formulation

2.1. Local plasma approximation

In their establishment of the LPA, Lindhard and Scharff (1953) argued that each small region of electron density in an atom contributes independently to the oscillator frequency and oscillator strength. They pointed out that there were two dominant frequencies associated with the electron density $n(r)$ at position r, namely the revolution frequency, W_n, of the independent-electron model and the plasma resonance frequency, $W_p(r) = [4\pi n(r)]^{1/2}$, of the electron gas model. They used a simple statistical model of atoms to show that these two frequencies were approximately equal in magnitude. Thus, it was concluded that the effective oscillation frequency, i.e. the square root of the sum of the two squared frequencies, was equal to $\gamma W_p(r)$ where $\gamma = \sqrt{2}$. The mean excitation energy of the atom, I, was then evaluated by averaging the space-varying effective oscillation energy according to the spherically symmetric electron density distribution, $4\pi r^2 n(r)$, of the atom. Actually, due to the definition of the mean excitation energy, the above averaging process should be carried out with the logarithm of the mean excitation energy. Hence, the logarithm of the mean excitation energy is expressed in the LPA as

$$\ln I = \frac{1}{Z} \int 4\pi r^2 n(r) \ln(\gamma W_p(r)) \, dr. \tag{2}$$

The above procedure may be applied to other physical quantities. This procedure is much easier than solving the complex transition matrix elements involving detailed atomic wavefunctions. Previous applications include several important physical parameters such as the mean excitation energy (Chu and Powers 1972, Tung and Watt 1985), the inelastic mean free path (Kwei and Chen 1988) and the stopping power (Tung *et al* 1979).

2.2. LPA *for a single-subshell atom*

In order to study the LPA, we consider first a dilute gas composed of atoms having a single subshell of binding energy W_b. The dynamic response function of the system is given by its dielectric function described by a bound electron gas model (Raether 1980)

$$\varepsilon(W) = \varepsilon'(W) + i\varepsilon''(W) = 1 + \frac{W_p^2}{W_b^2 - W^2 - i\Gamma W} \tag{3}$$

where $W_p = (4\pi n)^{1/2}$ is the free electron plasma energy associated with the collective oscillation, Γ is the plasma oscillation damping coefficient, and ε' and ε'' are the real and imaginary parts of the dielectric function, respectively. Note that the threshold excitation energy is W_b, or $W > W_b$. In other words, equation (3) is applicable only to transitions into the continuum states (ionisations) but not the discrete states (excitations) of atoms. We shall postpone our discussion about the contribution of excitations to the total GOS until § 2.4.

The effective oscillation or plasma energy of the bound electron system, $\tilde{W}_p$, defined as the resonance energy in the energy loss spectrum in the case of no plasma damping, is obtained by setting $\Gamma = 0$ in the equation $\varepsilon' = 0$. It is found that

$$\tilde{W}_p = (W_p^2 + W_b^2)^{1/2}. \tag{4}$$

This relation is in agreement with the statement of Lindhard and Scharff (1953), i.e. plasma and revolution frequencies share an equal contribution to the effective oscillation frequency.

In order to test the argument of Lindhard and Scharff concerning the equivalence in magnitude of W_p and W_b, we plot in figure 1 these two energies for the 1s and 2s subshells of a beryllium atom. The free electron plasma energy was computed using the electron density distribution from the Hartree-Fock-Slater model (Herman and Skillman 1963). It is clear from this figure that Lindhard and Scharff's argument is correct only in a gross average sense. In reality, the free electron plasma energy varies with the position of electrons because of the space-varying electron density, whereas

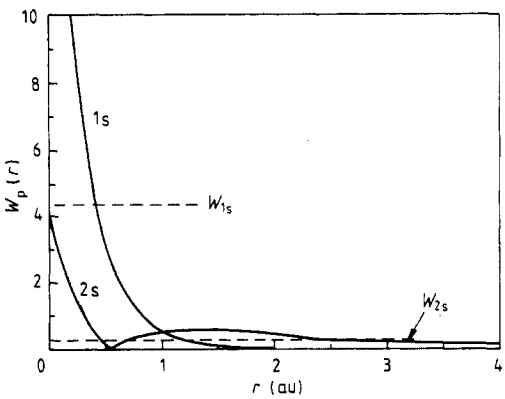

Figure 1. A plot of the free electron plasma energy for the 1s and 2s subshells of the beryllium atom as a function of the radial distance from the nucleus. The binding energies of the corresponding subshells are indicated by broken lines. All quantities are in atomic units.

the binding or revolution energy keeps a constant value at any position due to the quantisation of atomic orbitals.

The energy loss function, which is the imaginary part of the negative inverse dielectric function, is obtained using equations (3) and (4) as

$$\mathrm{Im}\left(-\frac{1}{\varepsilon(W)}\right)=\frac{W_{\mathrm{p}}^2 W\Gamma}{(W^2-\tilde{W}_{\mathrm{p}}^2)^2+W^2\Gamma^2}. \tag{5}$$

If we neglect plasma damping, i.e. $\Gamma=0$, the energy loss function becomes

$$\mathrm{Im}\left(-\frac{1}{\varepsilon(W)}\right)=\frac{\pi}{2}\frac{W_{\mathrm{p}}^2}{\tilde{W}_{\mathrm{p}}}\delta(W-\tilde{W}_{\mathrm{p}}) \tag{6}$$

Equation (6) was derived with the aid of the sum rule (Smith and Shiles 1978)

$$\int_0^\infty W\,\mathrm{Im}\left(-\frac{1}{\varepsilon(W)}\right)\mathrm{d}W=\frac{\pi}{2}W_{\mathrm{p}}^2. \tag{7}$$

Applying equations (1)-(6), we obtain

$$\mathrm{d}f/\mathrm{d}W=Z\delta(W-\tilde{W}_{\mathrm{p}}). \tag{8}$$

Equation (8) represents an infinitely sharp excitation spectrum for the system when neglecting the plasma damping.

In the LPA procedure, equation (8) should be averaged over the entire space according to the spherically symmetric electron density distribution $4\pi r^2 n(r)$. Following this procedure, we get the average GOS as

$$\frac{\mathrm{d}\bar{f}}{\mathrm{d}W}=\int 4\pi r^2 n(r)\delta(W-\tilde{W}_{\mathrm{p}}(r))\,\mathrm{d}r. \tag{9}$$

This result is the same as that derived by Johnson and Inokuti (1983) except for the replacement of $\gamma W_{\mathrm{p}}(r)$ by the effective plasma energy $\tilde{W}_{\mathrm{p}}(r)$. Equation (9) may be simplified to

$$\frac{\mathrm{d}\bar{f}}{\mathrm{d}W}=\sum_j\frac{4\pi r_{0j}{}^2 n(r_{0j})}{|\tilde{W}'_{\mathrm{p}}(r_{0j})|} \tag{10}$$

where $\tilde{W}'_{\mathrm{p}}(r_{0j})$ is the derivative of $\tilde{W}_{\mathrm{p}}(r)$ at r_{0j} and the r_{0j} are the roots of the equation

$$W-\tilde{W}_{\mathrm{p}}(r)=0. \tag{11}$$

2.3. LPA *for an atom with several subshells*

For a dilute gas composed of atoms having several subshells with different binding energies, the dielectric function of the system is given by

$$\varepsilon(W)=1+\sum_{\substack{i\\(W>W_i)}}\frac{W_{pi}^2}{W_i^2-W^2-i\Gamma_i W} \tag{12}$$

where $W_{\mathrm{p}i}$, W_i and Γ_i are, respectively, the free electron plasma energy, the binding energy and the plasma damping coefficient associated with the ith subshell. Note that each term in the summation of equation (12) is contributed by a given subshell. The restrictive condition $W>W_i$ ($i=1\mathrm{s}, 2\mathrm{s}, 2\mathrm{p}, \ldots$) must be satisfied by that subshell. The effective plasma energy, $\tilde{W}_{\mathrm{p}}$, of this system is again determined from the equation

$\varepsilon' = 0$ by setting $\Gamma_i = 0$. It can be shown that this energy is the solution of the equation

$$\prod_i (W_i^2 - \tilde{W}_{pi}^2) + \sum_i \left[W_{pi}^2 \left(\prod_{j \neq i} (W_j^2 - \tilde{W}_{pi}^2) \right) \right] = 0. \tag{13}$$

The subscript associated with the effective plasma energy indicates that there are many solutions of equation (13), actually as many as the number of subshells. In the case of a single subshell, equation (13) reduces to equation (4).

A comparison of the effective plasma energies calculated using the Lindhard and Scharff model, i.e. γW_p, the single or isolated subshell model of equation (4) and the multiple subshell model of equation (13) is made in figures 2 and 3 for oxygen 1s and 2p subshells. The electron density distributions have been obtained again from the Hartree-Fock-Slater model. It is seen that the effective plasma energies for the isolated and multiple subshell models show almost no difference in the case of the 1s shell but a substantial difference in the case of the 2p subshell. This is because electrons in the tightly bound 1s shell are relatively isolated and thus weakly correlated with electrons in other shells of the atom. Therefore, the isolated model works fairly well for the 1s shell. At large radii, the effective plasma energies for the Lindhard and Scharff model vanish whereas they approach the binding energies for the other two models. Because electrons in a given subshell cannot be excited (actually ionised) unless the excitation energy is greater than the binding energy of that subshell, it is evident that the Lindhard and Scharff model fails to describe the correct excitation behaviour at large radii.

Using equations (12) and (13), we are able to show that

$$\mathrm{Im}\left(-\frac{1}{\varepsilon(W)} \right) = \sum_i \frac{(\tilde{W}_{pi}^2 - W_i^2) W \Gamma_i}{(W^2 - \tilde{W}_{pi}^2)^2 + W^2 \Gamma_i^2}. \tag{14}$$

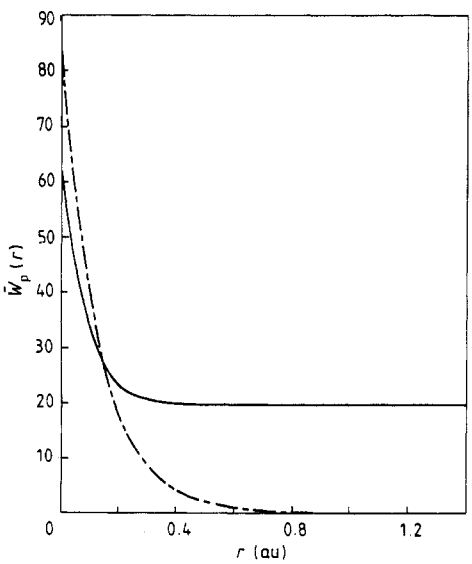

Figure 2. A plot of the effective plasma energy for the 1s shell of the oxygen atom as a function of the radial distance from the nucleus. The full curve is the result of the isolated-subshell model and the multiple-subshell model of the present work. The chain curve is the result of the Lindhard and Scharff (1953) model. All quantities are in atomic units.

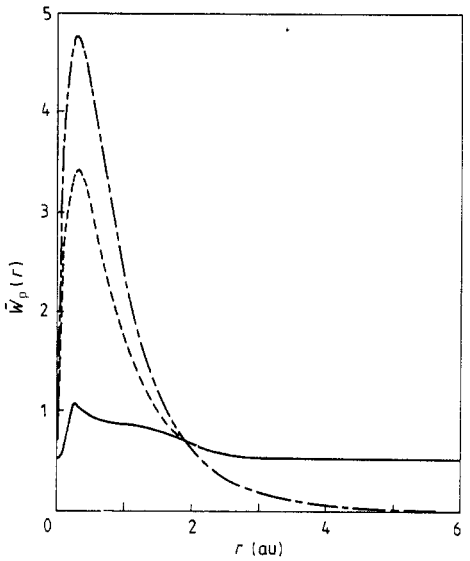

Figure 3. A plot of the effective plasma energy for the 2p subshell of the oxygen atom as a function of the radial distance from the nucleus. The full curve is the result of the multiple-subshell model. The broken curve is the result of the isolated-subshell model. The chain curve is the results of the Lindhard and Scharff (1953) model. Note that the broken curve coincides with the full curve for $r > 2$. All quantities are in atomic units.

Equation (14) is very useful because of its decoupled form into the summation over individual contributing terms. However, an explanation is required before the application of equations (13) and (14). Due to the restrictive condition imposed on each term in the summation of equation (12), equation (13) is also restrictive in the following way. Consider an atom composed of three subshells of binding energies W_1, W_2 and W_3 with $W_1 < W_2 < W_3$. In the excitation energy region $W > W_1$ and $W < W_2$, W_3, the second and third subshells do not contribute to the dielectric function of equation (12). Hence, in solving the effective plasma energy $\tilde{W}_{p1}$ using equation (13) these two subshells should not be taken into consideration. Similarly, the third subshell should be excluded from equation (13) when finding the effective plasma energy $\tilde{W}_{p2}$ in the region $W > W_1$, W_2 and $W < W_3$. Finally, we need to consider all three subshells in equation (13) to obtain $\tilde{W}_{p3}$ in the region $W > W_1$, W_2, W_3. Substituting $\tilde{W}_{p1}$, $\tilde{W}_{p2}$ and $\tilde{W}_{p3}$ into equation (14), we can show the agreement between the energy loss function calculated using this equation and that using equation (12) and the relation $\mathrm{Im}(-1/\varepsilon) = \varepsilon''/(\varepsilon'^2 + \varepsilon''^2)$.

We may rewrite equation (14) in a form similar to that of equation (5) by defining

$$\bar{W}_{pi}^2 = 4\pi\bar{n}_i = \tilde{W}_{pi}^2 - W_i^2. \tag{15}$$

Combining equations (14) and (15), we obtain

$$\mathrm{Im}\left(-\frac{1}{\varepsilon(W)}\right) = \sum_i \frac{\bar{W}_{pi}^2 W\Gamma_i}{(W^2 - \tilde{W}_{pi}^2)^2 + W^2\Gamma_i^2}. \tag{16}$$

If we neglect the plasma damping, i.e. take $\Gamma_i = 0$, we get

$$\mathrm{Im}\left(-\frac{1}{\varepsilon(W)}\right)_i = \frac{\pi}{2}\frac{\bar{W}_{pi}^2}{\tilde{W}_{pi}}\delta(W - \tilde{W}_{pi}) \tag{17}$$

where $\mathrm{Im}(-1/\varepsilon)_i$ is the energy loss function contributed by the ith subshell. Repeating the same analysis leading to equations (8)-(11), the GOS contributed by the ith subshell in the LPA can be obtained.

It is interesting to compute the number of electrons per atom contributing to the energy loss function up to an excitation energy W, i.e. $Z_e(W)$. This may be done by using equations (15) and (17). Recalling that $\tilde{W}_{pi}$ spans the region $W_i < W < W_{i+1}$, we obtain

$$Z_e(W) = \int_0^{r(W)} 4\pi r^2 n_i[\tilde{W}_{pi}(r)]\,\mathrm{d}r. \tag{18}$$

Figure 4 shows a plot of the results of $Z_e(W)$ for an aluminium atom using the electron density distribution from the Hartree-Fock-Slater model. For comparison, we have included in the figure results of similar calculations made by Smith and Shiles (1978) for solid aluminium.

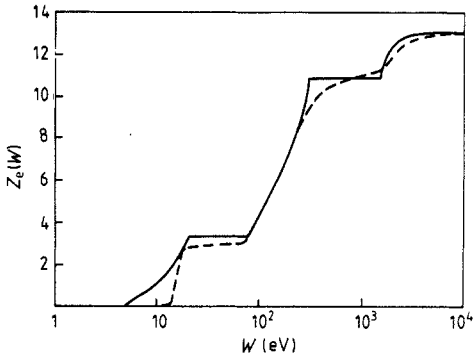

Figure 4. A plot of the number of electrons per atom contributing to the energy loss function up to an excitation energy W. The full curve is the result of present calculations for an aluminium atom. The broken curve is the result of Smith and Shiles (1978) for solid aluminium.

2.4. Plasma damping and GOS for ionisation

If we retain the plasma damping coefficient in equation (16), the delta function structure of the energy loss function does not exist any more. Instead, the energy loss spectrum becomes broadened with the width of the distribution proportional to the damping coefficient and the peak value around the effective plasma energy. Substituting equation (16) into equation (1) and applying the LPA procedure, we find

$$\frac{\mathrm{d}\bar{f}_i}{\mathrm{d}W} = \frac{2}{\pi}\int 4\pi r^2 n_i(r)\,\frac{W^2\Gamma_i}{[W^2 - \tilde{W}_{pi}^2(r)]^2 + W^2\Gamma_i^2}\,\mathrm{d}r. \tag{19}$$

The above derivation of GOS based on the LPA is valid for ionisations but not excitations of atoms. The GOS for discrete level transitions features a lineshape spectrum rather than the continuous spectrum for ionisations. Although in most cases ionisation is the dominant process responsible for the total oscillator strength, in other cases excitation may be of importance. In these latter cases, the use of the sum rule of equation (7) in the derivation of ionisation GOS should be corrected. Let F be the

fraction of the ionisation oscillator strength in the total oscillator strength. The above formulae for the ionisation GOS remain unchanged except that they should be multiplied by the fraction F.

3. Results and discussion

It is interesting to apply the single-subshell model of the LPA to a hydrogen atom which has one electron in the 1s shell with a binding energy of 1 Ryd (0.5 au). Substituting the electron density distribution (Harris 1975)

$$4\pi r^2 n(r) = 4\,\mathrm{e}^{-2r} r^2 \tag{20}$$

into equation (10), we get

$$\frac{d\bar{f}_{\mathrm{H}}}{\mathrm{d}W} = \frac{W}{4}\left(\ln\frac{4}{W^2 - \mathrm{Ryd}^2}\right)^2. \tag{21}$$

Figure 5 shows a comparison of the GOS for the hydrogen atom calculated using equation (21) and the hydrogenic wavefunction model (Merzbacher and Lewis 1958). Reasonably good agreement has been found. The GOS of the LPA vanishes for an excitation energy greater than 2 because of the neglect of plasma damping. Since the basic sum rule is satisfied in the LPA, its GOS is squeezed into the restricted region of $W < 2$.

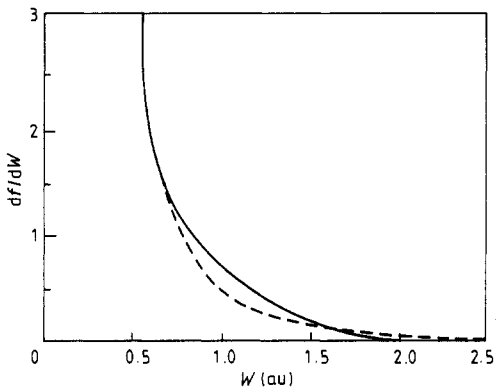

Figure 5. A comparison of the GOS for the hydrogen atom calculated using equation (21) (full curve) and the hydrogenic wavefunction model (broken curve) (Merzbacher and Lewis 1958). All quantities are in atomic units.

We now apply the multiple-subshell model to a two-subshell atom. Figure 6 shows a comparison of the GOS for the lithium atom calculated using equation (19) and the Hartree-Slater central potential model (McGuire 1971). The damping coefficients used for the 1s and 2s subshells are, respectively, 0.09 and 0.4. The oscillator strength fractions for ionisation of the respective subshells are 0.92 and 0.22 (Dehmer *et al* 1975). It is seen that the agreement between these two models is reasonably good. Application of the LPA reveals that the binding energy is responsible for the threshold behaviour of the GOS around this energy. The GOS at higher energies is mainly from the contribution of the plasma oscillation by local electron densities. The plasma

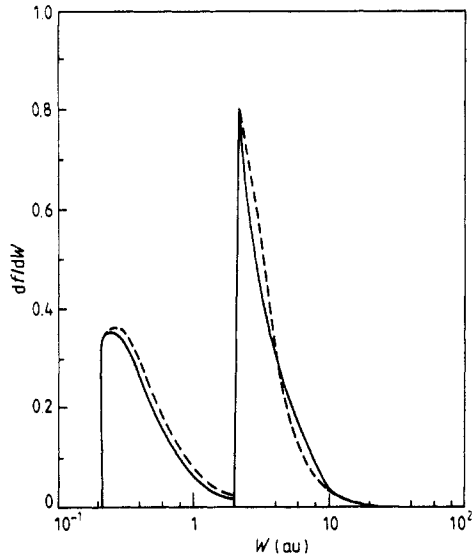

Figure 6. A comparison of the GOS for the lithium atom calculated using equation (19) (full curve) and the Hartree–Slater central-potential model (broken curve) (McGuire 1971). All quantities are in atomic units.

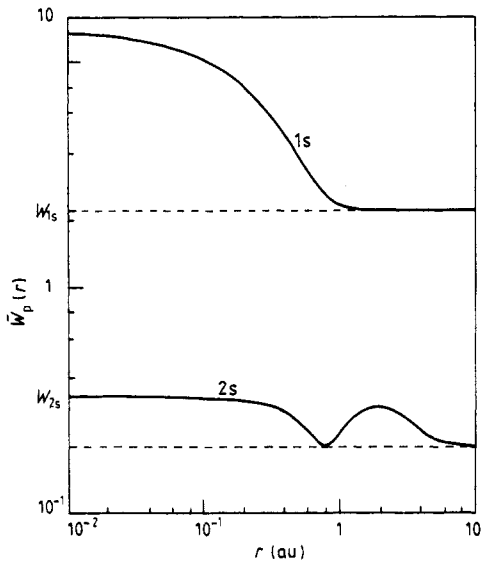

Figure 7. A plot of the effective plasma energy for the lithium atom as a function of the radial distance from the nucleus. Equation (13) was used for the calculations. Binding energies are indicated by the broken lines. All quantities are in atomic units.

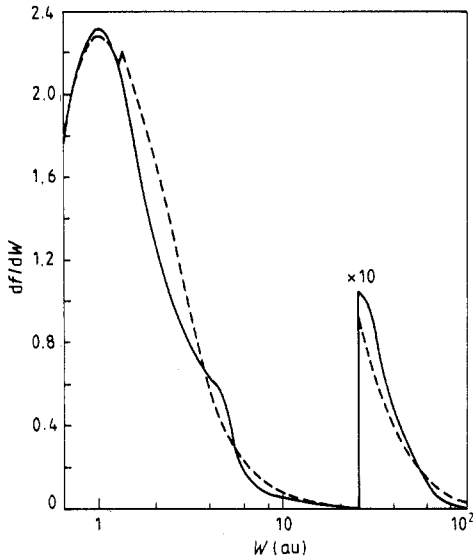

Figure 8. A comparison of the GOS for the fluorine atom calculated using equation (19) (full curve) and the Hartree–Slater central-potential model (broken curve) (McGuire 1971). The GOS values for the 1s shell have been multiplied by a factor of 10 for easy comparison. All quantities are in atomic units.

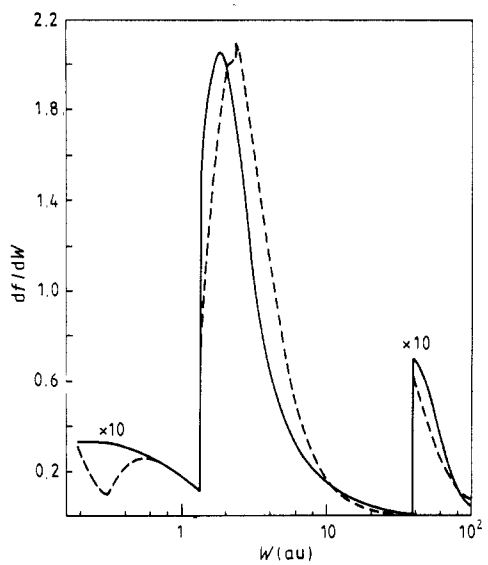

Figure 9. A comparison of the GOS for the sodium atom calculated using equation (19) (full curve) and the Hartree–Slater central-potential model (broken curve) (McGuire 1971). The GOS values for the 1s and 3s subshells have been multiplied by a factor of 10 for easy comparison. All quantities are in atomic units.

damping makes the GOS extend to very large excitation energies. This is understood from a plot of the effective plasma energy as shown in figure 7. The effective plasma energy approaches the binding energy at large radii where the electron density is very small. Therefore, the GOS corresponding to electrons at large radii shows the threshold behaviour around the binding energy. As the radius decreases, the effective plasma energy becomes gradually increasing due to the contribution from plasma oscillations. Since the effective plasma energy is finite everywhere, the GOS should vanish for excitation energies above the maximum effective plasma energy if no plasma damping is considered. It is this plasma damping which makes the GOS extend to infinite excitation energy.

Figure 8 shows a comparison of the GOS for the three-subshell fluorine atom calculated using equation (19) and the Hartree–Slater central-potential model (McGuire 1971). The damping coefficients used for the 1s, 2s and 2p subshells are 2.5, 1 and 1.27, respectively. The oscillator strength fractions for ionisation of the respective subshells are 0.96, 0.87 and 0.96 (Dehmer *et al* 1975). For the convenience of comparison, the GOS associated with the 1s shell has been multiplied by a factor of 10. Reasonably good agreement has also been found. A similar comparison for the four-subshell sodium atom is made in figure 9. Here the damping coefficients for the 1s, 2s, 2p and 3s subshells are 3.2, 10, 1.7 and 1, respectively. The oscillator strength fractions for ionisation of the respective subshells are 0.995, 0.988, 0.987 and 0.056. For the convenience of comparison, GOS associated with the 1s and 3s subshells have been multiplied by a factor of 10.

4. Conclusion

The LPA has proved in this work to be quite useful in predicting atomic GOS for ionisation. The basic idea and approach of Lindhard and Scharff have generally been followed. However, several modifications had to be made in order to obtain the correct features of the GOS spectrum. Firstly, quantum mechanical binding energies of individual subshells must be incorporated into the LPA to account for the threshold structures around these energies. The effective plasma energies must be determined by an equation involving binding energies and local plasma energies of all subshells.

The damping of plasma oscillation is important in the application of the LPA for GOS. It is generally felt that the damping coefficient is inversely proportional to the binding energy (Kliewer and Raether 1973). However, an examination of the GOS of the Hartree–Slater central potential model (McGuire 1971) reveals that the magnitude of this coefficient varies from subshell to subshell and from atom to atom. For the purpose of this work, we have merely treated this coefficient as a fit parameter. A detailed study of this parameter may be of interest.

References

Bethe H 1930 *Ann. Phys., Lpz* **5** 325
—— 1933 *Handbuch der Physik* vol 24 (Berlin: Springer)
Bragg W H and Kleeman R 1905 *Phil. Mag.* **10** 318
Chu W K and Powers D 1972 *Phys. Lett.* A **40** 23
Dehmer J L, Inokuti M and Saxon R P 1975 *Phys. Rev.* A **12** 102
Fano U 1963 *Ann. Rev. Nucl. Sci.* **13** 1

Harris E G 1975 *Introduction to Modern Theoretical Physics* (New York: Wiley)
Herman F and Skillman S 1963 *Atomic Structure Calculations* (New York: Prentice-Hall)
Johnson R E and Inokuti M 1983 *Comment. At. Mol. Phys.* **14** 19
Kliewer K L and Raether H 1973 *Phys. Rev. Lett.* **30** 971
Kwei C M and Chen L W 1988 *Surf. Interf. Anal.* **11** 60
Lenard P 1895 *Ann. Phys., Lpz* **56** 255
Lindhard J and Scharff M 1953 *K. Danske Vidensk. Selsk. Mat.-Fys. Meddr.* **27** 1
McGuire E J 1971 *Phys. Rev.* A **3** 267
Merzbacher E and Lewis H W 1958 *Handbuch der Physik* vol 34 (Berlin: Springer)
Raether H 1980 *Excitation of Plasmons and Interband Transitions by Electrons* (*Springer Tracts in Modern Physics* vol 88) (Berlin: Springer) p 48
Rutherford E 1911 *Phil. Mag.* **21** 669
Smith D Y and Shiles E 1978 *Phys. Rev.* B **17** 4689
Thompson J J 1912 *Phil. Mag.* **23** 449
Tung C J, Ashley J C and Ritchie R H 1979 *Surf. Sci.* **81** 429
Tung C J and Kwei C M 1985 *Nucl. Instrum. Methods* B **12** 464
Tung C J and Watt D E 1985 *Radiat. Eff.* **90** 177